Visualization of Guided Wave Propagation by Scanning Nonlinear Airborne Ultrasound Source Technique Using Compressed Sensing

Fumiya Hamada[1‡], Kyosuke Shimizu[1], Ayumu Osumi[2*], and Youichi Ito[2]
([1]Grad. of Sci. & Tech., Nihon Univ.; [2]Coll. of Sci. & Tech., Nihon Univ.)

1. Introduction

We have studied the non-contact and non-destructive testing method using the scanning airborne ultrasound source technique (SAS)[1,2] and the nonlinear harmonic method (NHM)[3,4] as the method to efficiently test large metal plate-like structures. The testing time of the SAS depends on the number of measurement points. Therefore, the testing time can be shortened by reducing the number of measurement points. However, reducing the number of measurement points causes the problem of undetected defects. As the method to solve this problem, Donoho et al. have proposed the compressed sensing[5]. Applying the compressed sensing[6-8] to the SAS offers the potentially significant testing time reductions.

In this report, as the basic study, we investigated the visualization of the guided wave propagation by the scanning nonlinear airborne ultrasound source technique using the compressed sensing.

2. Applying compressed sensing

The compressed sensing is the method of the image reconstruction from the down-sampling data by using the sparsity of target images. In this method, a spatial frequency spectrum X is estimated by solving the L_1norm minimization problem shown in equation (1).

$$X = \mathrm{argmin}\,\|X\|_1 \quad \mathrm{s.t}\ \ y = \phi\Psi X_0. \qquad (1)$$

Here, y is a down-sampling data, ϕ is a random down-sampling matrix, and Ψ is a sparsifying transform matrix.

The flow of the compressed sensing for the SAS is shown below. First, a random down-sampling matrix (compression ratio M/N) is set based on the conditions of the measurement area and the measurement interval at full sampling. Here, N is the number of full sampling points, M is the number of random down-sampling points. Next, a measurement is performed according to the random down-sampling matrix. Harmonic components are extracted from the time waveforms acquired at each measurement coordinate using a bandpass filter. The amplitude information of the extracted harmonics is assigned to y. After that, a reconstructed image x is obtained by performing an inverse 2D discrete cosine transform of X. In this study, the alternating direction method of multipliers (ADMM)[9] was used as the method to obtain X from equation (1). In addition, the reconstructed results obtained by the compressed sensing were evaluated by comparing the full sampling results with the reconstructed results.

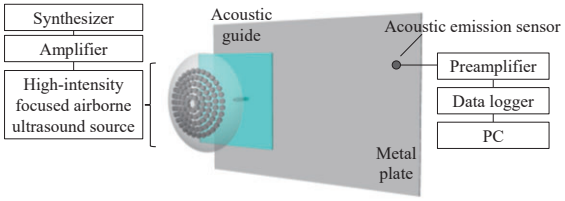

Fig. 1 Schematic of experimental equipment.

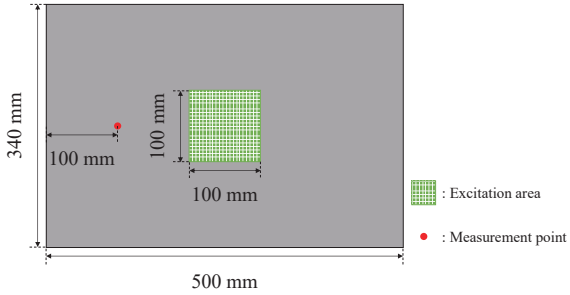

Fig. 2 Schematic of sample.

3. Experimental equipment and method

Figure 1 shows the schematic of the experimental equipment. The equipment was composed of a high-intensity focused airborne ultrasound source, an acoustic guide, an amplifier (HAS 4051: NF), a synthesizer (WF1974: NF), an acoustic emission (AE) sensor (PICO: Physical Acoustics), a preamplifier (2/4/6C: MISTRAS), a data logger (USB-6363: NI) and a PC that controls the peripheral equipment. The sound source is composed of 335 ultrasound emitters arranged on part of the spherical surface with a diameter of 150 mm. In addition, the sound waves were irradiated through the acoustic guide consisting of an acoustic window (acrylic; thickness: 2 mm) and a pipe

E-mail: *osumi.ayumu@nihon-u.ac.jp

(acrylic; length: 50 mm; inner diameter: 6 mm) to prevent the effects of side lobes. The sound source was driven by the burst wave with an applied voltage of 45 Vpp, a frequency of 40.8 kHz, and 10 cycles. The sound waves were irradiated under the above conditions contain integer-order harmonics in addition to the driving frequency because of nonlinear effects. Using these sound waves, harmonic imaging can be performed.

Figure 2 shows the schematic of the sample used in this experiment. The sample was made of the duralumin with dimensions of 500 × 340 × 3 mm.

Measurements were performed as follows. First, high-intensity focused sound waves from the sound source were irradiated to each position of the excitation area shown in Fig. 2 at intervals of 2 mm to excite guided waves in the sample. This vibration information was acquired by the AE sensor placed at the measurement position shown in Fig. 2. After that, the driving frequency (40.8 kHz), the second harmonic (81.6 kHz) and the third harmonic (122.4 kHz) were extracted from the time waveforms using the bandpass filter. Finally, reconstructed results were obtained by applying the compressed sensing process to randomly selected data (compression ratio: 25%) from the full sampling results.

The measurement conditions were the sampling frequency of 2 MHz, the sampling time of 5 ms, and the averaging process of 8 times.

4. Result

Figure 3-5 shows the guided wave propagation images from the fundamental to the third harmonics. Fig. (a) show the full sampling results and Fig. (b) show the reconstructed results. In addition, the results are normalized by the maximum value in each case.

First, the full sampling results shown in each Fig. (a) confirm that guided waves propagate in spherical shape. Next, in the reconstructed results shown in each Fig. (b), guided waves can also be seen propagating in spherical shape. In addition, the features of each Fig. (a) and each Fig. (b) are similar.

5. Conclusion

We reported on the visualization of the guided wave propagation by the scanning nonlinear airborne ultrasound source technique using the compressed sensing. As the results, it was confirmed that the propagation images could be reconstructed from 25% of the full sampling results.

In the future, we aim to detect defects in thin metal plates by using the SAS with applied the compressed sensing.

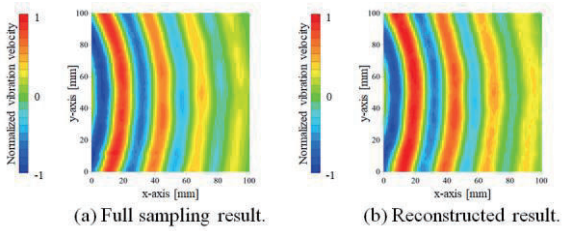

Fig. 3 Distribution of vibration velocity (40.8 kHz).

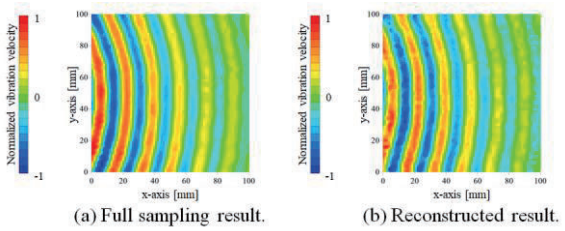

Fig. 4 Distribution of vibration velocity (81.6 kHz).

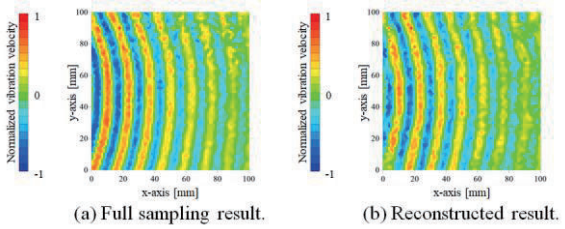

Fig. 5 Distribution of vibration velocity (122.4 kHz).

Acknowledgment

This work was partly supported by JSPS KAKENHI Grant number 22K04624.

References

1) K. Shimizu et al, Jpn. J. Appl. Phys., 59, SKKD15, 2020.
2) K. Shimizu et al, Jpn. J. Appl. Phys., 62, SJ1046, 2023.
3) A. Osumi et al, Jpn. J. Appl. Phys., 58, SGGB14, 2019.
4) A. Osumi et al, Acoust. Sci.& Tech., 41, pp. 885-890, 2020.
5) D. L. Donoho, in IEEE Transactions on Information Theory, 52, 4, pp. 1289-1306, 2006.
6) H. Song et al, Smart Mater. Struct., 29, 105011, 2020.
7) Y. Keshmiri Esfandabadi et al, in IEEE Transactions on Ultrasonics, Ferroelectrics, and Frequency Control, 65, 2, pp. 269-280, 2018.
8) T. Di Ianni et al, in IEEE Transactions on Ultrasonics, Ferroelectrics, and Frequency Control, 62, 7, pp. 1373-1383, 2015.
9) S. Boyd et al, Foundations and Trends in Machine Learning, 3, 1, 2010.